

Analysis of ICG Pharmacokinetics in Cancerous Tumors using NIR Optical Methods

Burak Alacam and Birsen Yazici
Dept. of Electrical, Computer,
Systems Engineering
Rensselaer Polytechnic Institute
Troy, New York 19102
Email: yazici@ecse.rpi.edu

Xavier Intes
ART Inc.
Saint-Laurent, Quebec
H4S 2A4 CANADA

Britton Chance
Department of Biochemistry and Biophysics,
University of Pennsylvania,
Philadelphia, PA 19104

Abstract— In this paper, we present three different compartmental models to model the pharmacokinetics of Indocyanine green (ICG) in cancerous tumors. We introduce a systematic and robust method to analyze ICG pharmacokinetics based on extended Kalman filtering (EKF) framework. We introduced information theoretic criteria for best compartmental model selection in terms of statistical fit. We tested our approach using the ICG concentration data acquired from four Fischer rats carrying adenocarcinoma tumor cells collected using near infrared (NIR) techniques. Our study indicates that, in addition to the pharmacokinetic rates and ICG concentrations in different compartments, EKF model may provide parameters that may be useful for cancerous tumor differentiation.

I. INTRODUCTION

Near infrared (NIR) diffuse optical imaging and spectroscopy methods provide quantitative functional information that cannot be obtained by the conventional radiological methods. At present, ICG is the only NIR optical agent approved for human use. Study of the time kinetics of ICG concentration curves may provide physiologically relevant information for tumor differentiation. Specifically, cancerous tissue types are expected to show high and fast uptake due to proliferation of "leaky" angiogenetic microvessels, while normal and fatty tissue show little uptake.

Current methods of ICG pharmacokinetic modeling involve curve fitting methods and various techniques for solving differential equations. Gurfinkel et. al. presented a two-compartmental model for ICG kinetics and estimated model parameters [1]. This study indicates that model parameters show no difference in the ICG uptake rates between normal and diseased tissue. Cuccia et al. presented a study of the dynamics of ICG in an adenocarcinoma rat tumor model [2]. A two-compartmental model describing the ICG dynamics is used to quantify physiologic parameters related to capillary permeability. The ICG concentration curves were fitted to the compartmental model using a non-linear least squares Levenberg-Marquart algorithm. It was shown that different tumor types have different capillary permeability rates. Intes et. al. presented the uptake of ICG by breast tumors using a continuous wave diffuse optical tomography apparatus [3]. A two-compartment model is used to analyze the pharmacokinetics of ICG. A curve fitting algorithm namely, non-linear Nelder-

Mead simplex search, is used to estimate the pharmacokinetic parameters. This study shows that the malignant cases exhibit slower rate constants as compared to healthy tissue.

While the studies described above demonstrate the feasibility of the ICG pharmacokinetics in tumor characterization; due to highly non-linear nature of the pharmacokinetic parameter estimation, variation in parameter values from one subject to another, and sparse data available in clinical and laboratory settings, a *systematic and robust* approach is needed to model, estimate and analyze ICG pharmacokinetics. Such an approach must include: *i*) a method for compartmental model order selection, *ii*) a robust method of estimating ICG pharmacokinetic parameters.

In this paper we present three different compartmental models for the ICG pharmacokinetics in cancerous tumors. We propose an extended Kalman filtering (EKF) framework to estimate the model parameters. We tested our approach using the ICG concentration data acquired from four Fisher rats carrying adenocarcinoma tumor cells. Two-, three- and four-compartment models are fitted to the data and pharmacokinetic model parameters and concentrations in different compartments are estimated using the EKF framework. Bayesian information criteria shows that the two-compartment model provides the best fit for our data. Estimated model parameters are used to differentiate between two different types of tumor. Our study suggests that the permeability rates are higher in edematous tumors as compared to necrotic tumors.

The paper is organized as follows: In Section II, we present the two-, three- and four-compartment models for the ICG pharmacokinetics in tissue. In Section III, we present the state-space representation of the compartmental models; estimation of ICG pharmacokinetics parameters and ICG concentrations in the EKF framework. In Section IV, we present optimal model order selection criteria, and the experimental results obtained from Fischer rat data. Section V summarizes our results and conclusion.

II. ICG PHARMACOKINETIC MODELING

A. Compartmental Analysis of ICG Pharmacokinetics

In this work we investigate three different compartmental models for the ICG kinetics and determine the optimal model

order based on Bayesian information criteria.

1) *The four-compartment model:* The four-compartment model includes capillary region, interstitial fluid region (ISF), parenchymal cell region, and intracellular binding site as compartments. The ICG injected intravenously into the subject can pass through from capillary into reversible binding site inside the cell through the ISF and the parenchymal cell region. Moreover, in advanced tumor stages, the leakiness around the tumor vessels is expected to increase resulting in higher permeability rates during the transportation of ICG into the compartments.

Let C_p , C_i , C_{pc} , C_b denote the ICG concentrations in plasma, ISF, parenchymal cell region and intracellular binding site, respectively; and let k_{out} , k_a , k_b , k_c , k_d , k_e and k_f be the constants used as equilibrium coefficients. Then the set of differential equations representing the ICG transition between the four compartments are given as follows:

The leakage into and the drainage out of plasma:

$$\frac{dC_p(t)}{dt} = k_b C_i(t) - k_a C_p(t) - k_{out} C_p(t). \quad (1)$$

The leakage into and the drainage out of ISF:

$$\frac{dC_i(t)}{dt} = k_a C_p(t) - k_b C_i(t) - k_c C_i(t) + k_d C_{pc}(t). \quad (2)$$

The leakage into and the drainage out of parenchymal cell:

$$\frac{dC_{pc}(t)}{dt} = k_c C_i(t) - k_d C_{pc}(t) - k_e C_{pc}(t) + k_f C_b(t). \quad (3)$$

The leakage into and the drainage out of intracellular binding site:

$$\frac{dC_b(t)}{dt} = k_e C_{pc}(t) - k_f C_b(t). \quad (4)$$

Physiologically, the equilibrium constants are defined by the permeability surface area products given as $PS\rho$, where P is the capillary permeability constant, S is the capillary surface area, and ρ is the tissue density. k_{out} is proportional to the flow rate into and out of the capillary and k_a , k_b , k_c , k_d , k_e , and k_f represent intra-tissue physiologic effects during ICG delivery from capillary to binding site.

The actual bulk ICG concentration in the tissue measured by NIR spectroscopy, $m(t)$, is a linear combination of the ICG concentrations in four different compartments.

$$m(t) = v_p C_p(t) + v_i C_i(t) + v_{pc} C_{pc}(t) + v_b C_b(t), \quad (5)$$

where v_p , v_i , v_{pc} , v_b , are volume fractions of plasma, ISF, parenchymal cell region and intracellular binding site, respectively.

2) *The three-compartment model:* In this model, the parenchymal cell and intracellular binding site compartments are combined to form a single compartment called parenchymal cell. This amounts to the assumptions that the transition of ICG into the intracellular binding site is negligible as compared to the other compartments and therefore omitted from the model.

3) *The two-compartment model:* In the two-compartment model, the tumor region is assumed to be composed of two compartments; namely, the capillary region and ISF. The transition of the ICG to the third and fourth compartments are assumed to be negligible. Therefore the last two compartments in the four compartment model is omitted. We consider transcapillary leakage to occur only at the tumor site. We also assume that a small perturbation of the global plasma concentration does not affect the bulk removal. The block diagrams of the compartmental transport and chemical model of ICG delivery for four, three, and two-compartment models are shown in Fig. 1(a), (b), and (c), respectively.

III. EXTENDED KALMAN FILTERING FOR THE ICG PHARMACOKINETICS

A. State-space Representation of the the ICG Pharmacokinetics

Coupled differential equations resulting from the compartment modeling of the ICG pharmacokinetics can be expressed in state-space representation as follows:

$$\begin{aligned} d\mathbf{C}(t) &= \kappa(\boldsymbol{\alpha}_n)\mathbf{C}(t)dt + \boldsymbol{\omega}(t)dt, \\ m(t) &= V(\boldsymbol{\alpha}_n)\mathbf{C}(t) + \eta(t). \end{aligned} \quad (6)$$

In (6), $\mathbf{C}(t)$ denotes the concentration vector; $\kappa(\boldsymbol{\alpha}_n)$ is the KF system matrix, $V(\boldsymbol{\alpha}_n)$ is the KF measurement matrix and $\boldsymbol{\alpha}_n$ is the parameter vector whose elements are the pharmacokinetic constants and the volume fractions for the n -compartment model, for $n = 2, 3, 4$.

The ICG measurements in (6) are collected at discrete time instances, $t = kT$, $k = 0, 1, \dots$, where T is the sampling period. Therefore, the continuous model described in equations (6) has to be discretized. To simplify our notation, we shall use $\mathbf{C}(k) = \mathbf{C}(kT)$ and $\mathbf{m}(k) = \mathbf{m}(kT)$. The discrete KF system and the measurement models are given as follows:

$$\begin{aligned} \mathbf{C}(k+1) &= \kappa_d(\boldsymbol{\alpha}_n)\mathbf{C}(k) + \boldsymbol{\omega}(k) \\ \mathbf{m}(k) &= V_d(\boldsymbol{\alpha}_n)\mathbf{C}(k) + \eta(k), \end{aligned} \quad (7)$$

where $\kappa_d(\boldsymbol{\alpha}_n) = e^{\kappa(\boldsymbol{\alpha}_n)}$ is the discrete-time KF system matrix and $V_d(\boldsymbol{\alpha}_n) = V(\boldsymbol{\alpha}_n)$ is the discrete-time KF measurement matrix. $\boldsymbol{\omega}(k)$ and $\eta(k)$ are zero mean Gaussian white noise processes with covariances matrix Q_d and variance σ_d^2 , respectively. To simplify the estimation process, we shall first estimate the matrix entries of the discrete-time system matrix $\kappa_d(\boldsymbol{\alpha}_n)$ and then compute the pharmacokinetic parameters for each compartmental model.

B. Modeling of ICG pharmacokinetic parameters and concentrations in extended Kalman filter framework

We consider a Taylor series approximation to the non-linear system function at the previous state estimates and that of the measurement function at the corresponding predicted position. A detailed discussion on Kalman filtering can be found in [4].

Let $\boldsymbol{\theta}_n(k)$ denote the discrete-time parameter vector of the pharmacokinetic rates and volume fractions at time k . In the

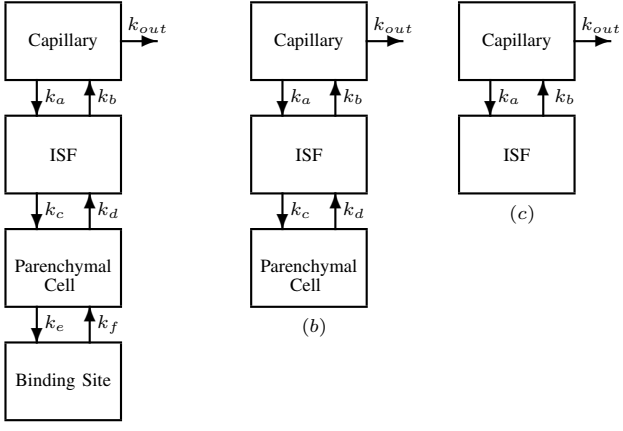


Fig. 1. Block diagrams of the (a) four-compartment, (b) three-compartment, (c) two-compartment models for the ICG pharmacokinetics.

EKF framework, $\theta_n(k)$ is treated as a random process with the following model:

$$\theta_n(k+1) = \theta_n(k) + \varsigma(k), \quad (8)$$

where $\varsigma(k)$ is a zero mean white noise process with covariance matrix S_d .

We append the parameter vector $\theta_n(k+1)$ to the ICG concentration vector $\mathbf{C}(k+1)$ to form the new non-linear state-space model given as

$$\begin{bmatrix} \mathbf{C}(k+1) \\ \theta_n(k+1) \end{bmatrix} = \begin{bmatrix} \mathbf{K}(\theta_n)\mathbf{C}(k) \\ \theta_n(k) \end{bmatrix} + \begin{bmatrix} \omega(k) \\ \varsigma(k) \end{bmatrix} \quad (9)$$

$$\mathbf{m}(k) = [V_d(\theta_n) \ 0] \begin{bmatrix} \mathbf{C}(k) \\ \theta_n(k) \end{bmatrix} + \eta(k),$$

where $\mathbf{K}(\theta_n) = \kappa_d(\alpha_n)$.

C. EKF joint estimation for ICG concentrations, pharmacokinetic parameters, and volume fractions

In this section we will summarize the major steps of the EKF estimator for the joint estimation of ICG concentrations and compartmental model parameters.

Let the subscript $k|t$ denote the estimate at time k given all the measurements up to time t . Then the 1-step ahead prediction of the ICG concentrations and the compartmental model parameters are given as follows:

$$\begin{bmatrix} \hat{\mathbf{C}} \\ \hat{\theta}_n \end{bmatrix}_{k|k-1} = \begin{bmatrix} \mathbf{K}(\hat{\theta}_n)\hat{\mathbf{C}} \\ \hat{\theta}_n \end{bmatrix}_{k-1|k-1}. \quad (10)$$

The error covariance matrix, $P_{k|k-1}$, of the 1-step ahead predictions is given as follows:

$$P_{k|k-1} = J_{k-1} P_{k-1|k-1} J_{k-1}^T + \begin{bmatrix} Q_d & 0 \\ 0 & S_d \end{bmatrix}, \quad (11)$$

where J_k is the Jacobian of the non-linear EKF system function at time k . Explicitly, it is given as:

$$J_k = \begin{bmatrix} \mathbf{K}(\hat{\theta}_n) & \frac{\partial}{\partial \theta_n} [\mathbf{K}(\hat{\theta}_n)\hat{\mathbf{C}}] \\ \mathbf{0} & \mathbf{I} \end{bmatrix}_{k|k}, \quad (12)$$

where $\mathbf{0}$ and \mathbf{I} denote zero and identity matrices, respectively.

The 1-step ahead predictions are updated to the k^{th} -step estimates by means of the Kalman gain matrix which is given by

$$G_k = P_{k|k-1} \Lambda^T [\Lambda P_{k|k-1} \Lambda^T + \sigma_k^2]^{-1}, \quad (13)$$

where Λ is the following vector

$$\left[\begin{array}{cc} V_d(\hat{\theta}) & \frac{\partial}{\partial \theta} [V_d(\hat{\theta})\hat{\mathbf{C}}] \end{array} \right]_{k|k-1}. \quad (14)$$

The k^{th} -step estimate of the concentrations and the parameters are obtained recursively using

$$\begin{bmatrix} \hat{\mathbf{C}} \\ \hat{\theta} \end{bmatrix}_{k|k} = \begin{bmatrix} \hat{\mathbf{C}} \\ \hat{\theta} \end{bmatrix}_{k|k-1} + G_k (\mathbf{m}(k) - [V_d(\hat{\theta})\hat{\mathbf{C}}]_{k|k-1}). \quad (15)$$

The error covariance matrix, $P_{k|k}$, of the k^{th} -step estimates is updated as

$$P_{k|k} = [I - G_k \Lambda] P_{k|k-1}, \quad (16)$$

where \mathbf{I} is the identity matrix.

IV. EXPERIMENTAL RESULTS

We applied the proposed EKF framework to the pharmacokinetic analysis of ICG data obtained from four Fischer rats with adenocarcinoma. R3230ac adenocarcinoma cells were injected below the skin into four Fischer rats. The ICG concentration data was collected with an MRI-NIR imager. The configuration of the apparatus and the detailed data collection procedure have been reported in [2]. Tumors in Rat 1 and 2 are classified as necrotic because of their low tissue oxy-hemoglobin, low total hemoglobin, and low gadolinium-diethylene-triamine penta-acetic acid (Gd-DTPA) enhancement levels. Tumors in Rat 3 and 4 are classified as edematous due to their high water content.

Based on the model parameter estimates, we adopted Bayesian information criteria (BIC) for the optimal model order selection. A detailed discussion on BIC can be found in [5]. In order to calculate the BIC for different compartmental models, we first derived a likelihood function for the extended Kalman filter. The derivation is based on the maximum likelihood estimation of the parameters in the Kalman filtering framework. We then modified this likelihood function for the extended Kalman filter estimator for the joint estimation of compartmental model parameters and concentrations. The BIC values and the number of unknown parameters for each rat data are tabulated in Table I. The BIC suggests that the two-compartment model is the statistical best model and sufficient for all four measurement sets.

In order to characterize the difference between these two tumors, we estimated the pharmacokinetic parameters k_a , k_b and k_{out} , and the volume fractions v_p and v_i for each rat in the two-compartment model. Table 2 tabulates the estimated parameters. The rate of leakage into the ISF from the capillary, k_a , range from 0.0247 to 0.0840 sec⁻¹ and the rate of drainage out of the ISF and into the capillary, k_b , range from 0.0106 to 0.0777 sec⁻¹. Note that the permeability rates

TABLE I

TEST FOR THE MODEL ORDER SELECTION FOR THREE DIFFERENT COMPARTMENTAL MODELS FOR FOUR DIFFERENT DATA SETS

Model	p	Rat1 $\phi_{BIC}(p)$	Rat2 $\phi_{BIC}(p)$	Rat3 $\phi_{BIC}(p)$	Rat4 $\phi_{BIC}(p)$
Two-comp.	7	-178.242	-198.367	-202.81	-172.098
Three-comp.	11	-71.615	-83.849	-92.182	-63.912
Four-comp.	15	-39.719	-45.121	-56.340	-30.023

TABLE II

TWO-COMPARTMENT MODEL: ESTIMATED PHARMACOKINETIC PARAMETERS AND VOLUME FRACTIONS USING EKF ALGORITHM

	$k_a(\text{sec}^{-1})$ (10^{-2})	$k_b(\text{sec}^{-1})$ (10^{-2})	$k_{out}(\text{sec}^{-1})$ (10^{-3})	v_i (10^{-2})	v_p (10^{-2})
Rat 1	2.47	1.06	4.61	21.8	1.41
Rat 2	3.54	2.98	4.83	25.4	2.42
Rat 3	6.90	4.93	3.95	30.4	4.84
Rat 4	8.40	7.77	4.02	53.0	7.03

for the necrotic cases are lower than the ones observed for the edematous cases. Additionally, the estimated values for the pharmacokinetic rates are much higher than the normal tissue values due to the increased leakiness of the blood vessels around the tumor region. The estimated plasma volume fractions agrees with the values reported earlier [2]. These results confirm that v_p can be significantly large in tumors and that its magnitude varies with respect to the stage of the tumor. The estimated values of ISF volume fraction, v_i , range from 0.218 to 0.53, in agreement with 0.2 to 0.5 range reported earlier [6]. Note that these results are valid only for the ICG pharmacokinetics in tumor cells R3230ac, adenocarcinoma and may not be generalized for other types of contrast agents or tumor types.

Fig. 2 shows the estimated ICG concentrations in the plasma and the ISF compartments for the two-compartment model for Rats 1 to 4. Note that initial estimates of concentrations are noisy due to the limited data used in the recursive EKF estimation. This can be improved by Kalman backward smoothing. The peak values of the plasma concentration, C_p , range from $2.72 \mu\text{M}$ to $4.28 \mu\text{M}$. The absolute value of the concentrations may not be very useful. However, concentration of ICG in one compartment relative to the concentration in another compartment may provide useful information. We consider the ratio of the peak concentrations in the plasma and ISF as a potential parameter to discriminate different tumors. The peak C_p/C_i ratio for Rats 1 to 4 is 0.551, 0.593, 0.787, 1.151, respectively. This ratio is higher in edematous cases consistent with the fact that ICG-albumin leaks more into the ISF in advanced tumors. Additionally, the ICG concentration in plasma decays faster than the ICG concentration in ISF due to ICG elimination through the liver and kidneys.

V. CONCLUSION

In this paper we present three different compartmental models and an extended Kalman filtering framework for

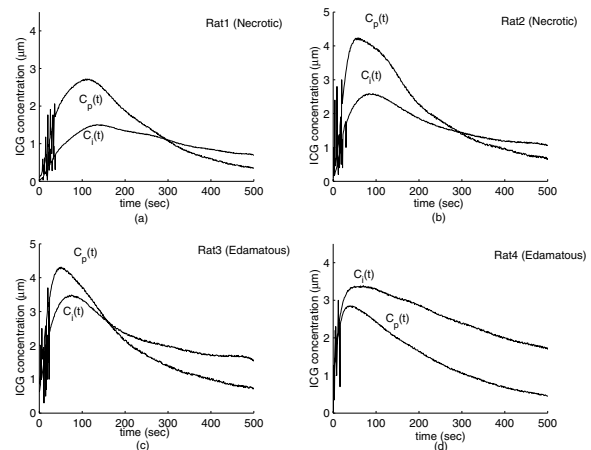


Fig. 2. ICG concentrations in plasma, $C_p(t)$ and ISF, $C_i(t)$, for four different rats. (a) Rat1, (b) Rat2, (c) Rat3, (d) Rat4.

the modeling and estimation of ICG pharmacokinetics in cancerous tumors based on NIR measurements. Additionally, we introduce information theoretic criteria for model selection. Proposed compartmental models are fit to data obtained from Fischer rats with adenocarcinoma cells. Based on the BIC analysis, we concluded that the two-compartment model provides the best statistical fit for the rat data. The two-compartment results indicate that the permeability rates are higher for the edematous tumors. Additionally, we estimated the ICG concentrations in different compartments. The concentrations in different compartments may provide additional parameters for tissue characterization. As a future work, we plan to use the EKF framework in the modeling and analysis of the pharmacokinetics of different optical contrast agents collected from animals and the ICG data collected from human subjects.

ACKNOWLEDGMENT

This work was supported by U.S. Army Medical Research Acquisition Activity under grant W81XWH-04-1-0559, and Office of Naval Research under grant N000014-04-1-0694. The Authors would like to thank Dr. Bruce Tromberg and Dr. David Cuccia for providing the rat data used in our study.

REFERENCES

- [1] M. Gurfinkel, A. B. Thompson, W. Ralston, T. L. Troy, A. L. Moore et al., "Pharmacokinetics of ICG and HPPH-car for the detection of normal and tumor tissue using fluorescence, near-infrared reflectance imaging: a case study," *Photochem. Photobiol.*, Vol. 72, 2000, pp. 94-102.
- [2] D.J. Cuccia, F. Bevilacqua, A. J. Durkin, S. Merritt, B. J. Tromberg et al., "In vivo quantification of optical contrast agent dynamics in rat tumors by use of diffuse optical spectroscopy with magnetic resonance imaging coregistration," *Applied Optics*, Vol. 42, No 1, June 2003.
- [3] X. Intes, J. Ripoll, Y. Chen, S. Nioka, A. G. Yodh, B. Chance, "In vivocontinuous-wave optical breast imaging enhanced with Indocyanine Green," *Med. Phys.* Vol. 30-6, June 2003.
- [4] C.K.Chui, G. Chen, *Kalman Filtering with real time applications*, Springer, Berlin, 1999.
- [5] G. Schwarz, "Estimating the dimensions of a model," *Annals of Statistics*, Vol. 6, pp. 461-464, 1978.
- [6] P. S. Tofts, DPhil, G. Brix, D. L. Buckley, J. L. Evelhoch et al., "Estimating Kinetic Parameters From Dynamic Contrast-Enhanced T1-Weighted MRI of a Diffusible Tracer: Standardized Quantities and Symbols," *Jour. Mag. Res. Im. Vol. 10*, pp. 223-232, 1999.